Constraining Spatial Curvature with Strong Gravitational Lenses and Complementary Probes: a Forecast for Next-Generation Surveys

Project Report

Author: Yang Hu
Supervisor: Dr. Suhail Dhawan

August 2022

Abstract

It is of great interest in cosmology to obtain a high-fidelity constraint on curvature density parameter Ω_k that is independent of the early universe Cosmic Microwave Background measurement. In this project, we explored the ability of using simulated time-delay distance measurement from next-generation survey on strong gravitational lenses to complement simulated next-generation surveys on type Ia supernovae and baryon acoustic oscillations on constraining Ω_k. We present a parametric method and also a non-parametric method to do so. In the parametric approach, we assumed an owCDM model and showed that the inclusion of strong gravitational lensing data into the analysis breaks the w-Ω_k degeneracy that existed in analysis with the two other probes' data, leading to a constrain on curvature: $\Omega_k = -0.003^{+0.014}_{-0.014}$. In the non-parametric approach, we used Gaussian Process regression for non-parametric inference of Hubble parameter H_z and obtained a constraint on curvature to be $\Omega_k = -0.0004^{+0.0139}_{-0.0142}$. This serves as a promising forecast for using next-generation surveys to constrain Ω_k.

1 Introduction

The curvature density parameter Ω_k determines the geometry of the universe, and a key interest in modern cosmology is to obtain a high-fidelity constraint on Ω_k that is independent of the early-universe Cosmic Microwave Background (CMB) measurement. There are many late-universe cosmological probes that impose constraint on curvature. Depending on the sensitivity of measurable quantities to variation in curvature, the strength of the constraint on Ω_k imposed by each probe differs significantly. Strong gravitational lenses (SGL), type Ia supernovae (SNe Ia), and baryon acoustic oscillations (BAO) are believed to be such kind of probes that impose constraint on Ω_k. Their respective measurable quantities are time-delay distance, apparent magnitude and Hubble parameter, and all of them are closly related to the curvature Ω_k together with other paramters such as Hubble's constant H_0 and matter density parameter Ω_m.

The constraint imposed on Ω_k by SGL, SNe Ia and BAO individually have been widely analysed and discussed in past literature. A promising study on constraining Ω_k is to combine a large number of time-delay distance measurements from SGL with SNe Ia and BAO, hoping that the combined data can overcome the deficiency of limited lensing events in previous analysis such as that by K. C. Wong et al. 2019[1] on 6 SGL events and degeneracies (see section 2.3) among cosmological parameters in single-probe analysis. In light of the next-generation survey from the Vera C. Rubin Observatory's legacy survey of space and time (LSST), it is expected that hundreds of SGL events will be observed during its 10-year survey baseline[2]. This will provide a large dataset for cosmologists to study the ability of SGL to constrain Ω_k. In this project, we present a parametric method and a non-parametric method to constrain Ω_k with simulated combined data of next-generation SGL surveys and complementary probes.

2 Methodology

2.1 Measurables in cosmology

It is helpful to recall how measurements from cosmological probes relate to and constrain cosmological parameters, where readers may have already encountered them in textbooks or other resources in cosmology. Nevertheless, we provide a summary of the relations between measurable quantities from SGL, SNe Ia and BAO and cosmological parameters of interests, especially the relations involving Ω_k.

For BAO at redshift z, the measurable quantity is the Hubble parameter H_z. In the case of parametric modelling of the universe in this project, we assumed an owCDM model, where o allows for non-flat geometry and w is the equation-of state parameter for dark energy. Then, H_z takes the following form:

$$H_z = H_0\sqrt{\Omega_m(1+z)^3 + \Omega_k(1+z)^2 + \Omega_{de}(1+z)^{3(1+w)}}, \tag{1}$$

where H_0 is the Hubble's constant, Ω_m is the matter density parameter and Ω_{de} is the dark energy

density parameter. Note that $\Omega_{de} = 1 - \Omega_m - \Omega_k$ so that the free cosmological parameters BAO try to constrain in the parametric case are only H_0, Ω_m, Ω_k and w.

For SNe Ia at redshift z, the measurable quantity is the apparent magnitude m_B given by:

$$m_B = 5\lg(D_L) + 25 + M_B, \tag{2}$$

where M_B is the absolute magnitude and D_L is the luminosity distances at z. D_L is given by:

$$D_L = \frac{c(1+z)}{H_0\sqrt{|\Omega_k|}} F\left(\sqrt{|\Omega_k|}\int_0^z \frac{\mathrm{d}z'}{E(z')}\right), \tag{3}$$

where function F is sin for $\Omega_k \leq 0$ and sinh for $\Omega_k > 0$. $E(z) = H_z/H_0$ is the normalised Hubble parameter. In the parametric case, the free cosmological parameters that SNe Ia try to constrain are $H_0, \Omega_m, \Omega_k, w$ and M_B.

For SGL with lens at redshift z_l and source at redshift z_s, the measurable quantity is the time-delay distances $D_{\Delta t}$ given by:

$$D_{\Delta t} = \frac{(1+z_s)D_{A,l}D_{A,s}}{D_{A,ls}}, \tag{4}$$

where $D_{A,l}$ and $D_{A,s}$ are angular diameter distances at lens and source respectively, and $D_{A,ls}$ is the angular diameter distance between lens and source. D_A at a particular redshift z can be calculated by $D_A = D_L/(1+z)$. Define $D_h = c/H_0$, and $D_{A,ls}$ can be calculated by the following equation:

$$\begin{aligned} D_{A,ls} =& \frac{1}{1+z_s}\left(\frac{D_{A,s}}{1+z_s}\sqrt{1+\Omega_k\left(\frac{D_{A,l}}{D_h(1+z_l)}\right)^2}\right. \\ &\left. -\frac{D_{A,l}}{1+z_l}\sqrt{1+\Omega_k\left(\frac{D_{A,s}}{D_h(1+z_s)}\right)^2}\right). \end{aligned} \tag{5}$$

In the parametric case, the free cosmological parameters that SGL try to constrain are H_0, Ω_m, Ω_k and w.

2.2 Markov chain Monte Carlo

Having known the equations that relate cosmological parameters of interests to measurable quantities, we now need a procedure to tell the strength of constraint that probes place on each parameter. In this project, the procedure adopted is Markow chain Monte Carlo (MCMC) sampling.

In Bayesian statistics, in order to know the posterior distribution of a parameter, we need a prior distribution based on current knowledge about the parameter and a likelihood function based on agreement between data and model. The product of the latter two is proportional to the former one, as stated in Bayes's Theorem. The MCMC sampler will draw samples of the cosmological parameter based on this posterior distribution (such that in theory, drawing infinitely many samples perfectly reconstruct the posterior distribution). Computationally, we used python package *emcee* to achieve

Table 1: Priors on free parameters

Parameter	**Prior**
H_0	U(0,150) km/s/Mpc
Ω_m	U(0.05, 0.5)
Ω_k	U(-0.5,0.5)
w	U(-2.5,0.5)
M_B	U(-38.4,0) mag

this. Once the posterior distribution curve of a parameter is obtained by drawing sufficiently many samples, we can read off the constraint on the parameter from the mean and standard deviation of the curve. The question reduces to what prior to assume for each cosmological parameter and what likelihood function to choose for each probe (which produces a comparison between data and model).

Past cosmological surveys have already suggested possible range or even precise values of the cosmological parameters. However, in this project, for the purpose of generality, we assumed conservative uniform priors for all the cosmological parameters of interests, where past literature values will approximately locate at the center of the distribution. They are shown in table 1.

The likelihood functions for all three probes take the form of χ^2 terms. The χ^2 accounts for the degree of 'disagreement' between data and model. For SGL, it is:

$$\chi^2_L = \sum_i \frac{(D_i - D_{m,i})^2}{\sigma^2_{D_i}}, \tag{6}$$

where D_i is the i^{th} time-delay distance measurement, σ_{D_i} is its percentage uncertainty and $D_{m,i}$ is the i^{th} modelled value calculated using equation (4) in the assumed owCDM universe.

For BAO, the χ^2 term takes a similar form:

$$\chi^2_B = \sum_i \frac{(H_i - H_{m,i})^2}{\sigma^2_{H_i}}, \tag{7}$$

where H_i is the i^{th} H_z measurement, σ_{H_i} is its percentage uncertainty and $H_{m,i}$ is the i^{th} modelled value of H_Z calculated using equation (1).

The χ^2 term of SNe Ia measurements take a different form:

$$\chi^2_S = \Delta \boldsymbol{m_B}^T \cdot \boldsymbol{C}^{-1} \cdot \Delta \boldsymbol{m_B}, \tag{8}$$

where $\Delta \boldsymbol{m_B} = \boldsymbol{m_B} - \boldsymbol{m_B}_{\text{model}}$ is a vector of difference between measured and modelled apparent magnitudes and $\boldsymbol{C} = \boldsymbol{D}_{\text{stat}} + \boldsymbol{C}_{\text{sys}}$ is the covariance matrix as a sum of the diagonal statistical uncertainty matrix and the systematic uncertainty matrix. The overall likelihood function will be the sum of individual χ^2 terms of probes used in the analysis. Now we have all necessary methodology for the parametric approach. The parametric approach directly use MCMC sampler on parameter-measurable equations in section 2.1 to constrain parameters.

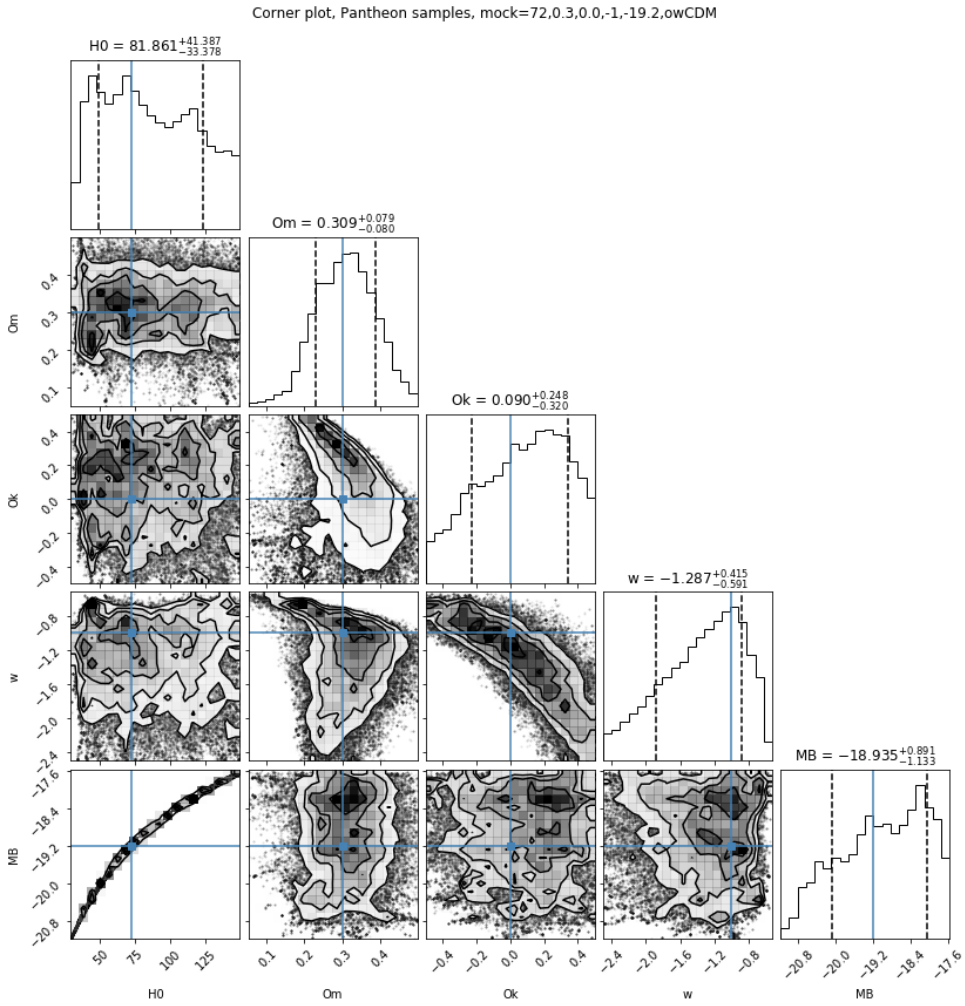

Figure 1: Constraint on parameters by past SNe Ia survey Pantheon

2.3 Degeneracies

Readers may worry that some relations in section 2.1 do not simultaneously constrain some parameters well. A well-known example is that for SNe Ia and their parameter-measurable equations (2) & (3), both H_0 and M_B enter the equations as additive terms. Therefore, it is almost equally likely for MCMC sampler to draw different values of (H_0, M_B) as long as their sums are the same. This is called a degeneracy. We used MCMC sampler on a past SNe Ia survey Pantheon with simulated binned data provide by D. M. Scolnic et al. 2018[3] to demonstrate the concept of degeneracy. In Fig. 1, the narrow but elongated M_B-H_0 contour at the bottom left of the corner plot suggests that both H_0 and M_B can take a range of values as long as they fall into the demarcated region, hence imposing weak constraints on H_0 and M_B. Degeneracy sets a fundamental limitation on using single-probe data to constrain cosmological parameters. To break degeneracy, we need to use multiple-probe data. It is also well-known that combining SGL data (which places a strong constraint on H_0) with SNe Ia breaks this degeneracy.

In the parametric approach, similar degeneracy exists between w and Ω_k in SNe Ia and BAO. This sets another limit on the ability of single-probe data to constrain Ω_k. This is the reason that we add SGL data into analysis, hoping that this break the w-Ω_k degeneracy in other probes. In the non-parametric approach which we will introduced later, w is no longer a parameter. Therefore, we do not need to worry about w-Ω_k degeneracy, yet H_0-M_B degeneracy still exists.

2.4 Gaussian Process Regression

A limitation of the parametric approach is that the Hubble parameter H_z in equation (1) depends heavily on what model of dark energy we assumed. In equation (1), we can seen that because we assumed an owCDM model, H_z then depends on free parameters H_0, Ω_m, Ω_k and w. If a different model, e.g $o\Lambda$CDM, is assumed, then H_z will no longer depend on w, and w will be replaced by -1 in equation (1). The form of the function H_z depends entirely on the choice of parameters. Since H_z appears everywhere in other relations, all measurable quantities depend heavily on the parameters we chose.

To lessen this parameter-dependency, an alternative method is to infer H_z non-parametrically. Instead of specifying the parameters that determine the form of H_z, we only assume the general characteristics of the H_z function and they are controlled by the so-called hyper-parameters. The general characteristics of the function are implied in covariance function $k(x_i, x_j)$ (or kernel) which tells the correlation between getting a measurement at x_j and a measurement at x_i. We assign a higher probability to functions with characteristics that match our prior knowledge about H_z. To do this systematically, Gaussian Process regression (GP) comes into play. A complete guide on GP can be found in Rasmussen & Williams 2006[4].

The key assumption of GP is that in a collection of random variables, any finite number of them satisfy a multivariate Gaussian distribution characterised by a mean function (which can be 0 for simplicity) and a kernel (just like the covariance matrix in a finite-dimensional Gaussian distribution). After choosing such a kernel, an interpolated curve of H_z at any z can be easily obtained by drawing samples from this multivariate Gaussian distribution. We know that H_z is a smoothly varying function of z, and the kernel should capture this characteristic. A common choice for smoothly varying function is the squared exponential kernel given by:

$$k_{SE}(x_i, x_j) = a^2 \exp\left(\frac{-(x_i - x_j)^2}{2l^2}\right), \tag{9}$$

where hyper-parameter a can be interpreted as the characteristic amplitude of H_z, and hyper-parameter l can be interpreted as the characteristic length-scale of z such that two measurements in H_z are strongly correlated. They are referred to as amplitude and length-scale in this project.

In this project, we used python package *george* to optimise the hyper-parameters for k_{SE} and perform GP. Once we obtained the non-parametrically interpolated H_z curved from *george*, we saw from equations (2) to (5) that the remaining unknowns among all three probes are only H_0, Ω_k and M_B, and MCMC can be applied on these three to constrain Ω_k. Non-parametric approach to constraint Ω_k with cosmic chronometers measurements and Pantheon SNe Ia data has been examine by S. Dhawan et al. 2021[5], where $\Omega_k = -0.03 \pm 0.26$ was obtained. We would expect

an improvement using data from next-generation surveys. For the purpose of comparison, this non-parametric approach using GP to constrain Ω_k will only be done later after which parametric analysis is completed first in the next section.

3 Parametric Analysis

3.1 Data generation and simulation

For parametric analysis, we assumed an owCDM model and set the mock universe with the following cosmological parameters: $H_0 = 72$ km/s/Mpc, $\Omega_m = 0.3, \Omega_k = 0, w = -1, M_B = -19.2$ mag. Such a mock universe is referred to as the standard setting in this project.

During the 10-year LSST survey, approximately 300 SGL events are expected to be observed. LSST DESC data products[6] provided 310 pairs of simulated (z_l, z_s) data, and they are referred to as LSST-like data in this project. LSST-like data are used to generate mock $D_{\Delta t}$ measurements using equation (4). We also generated the percentage uncertainty of each mock $D_{\Delta t}$ measurement as a random number between 6% to 10%. In the future, the number of effective SGL measurements can increase if quasars and other similar probes are taken into account. Therefore, we hoped to mimic the uncertainty of 3000 SGL measurements by multiplying each percentage uncertainty drawn by $\sqrt{310/3000}$. In the following analysis involving SGL, we used 310 SGL with reduced uncertainty (we call it '3000' lenses) to reduce computational cost when implementing MCMC. When MCMC samples are large, as is the case in this project, taking this shortcut is statistically equivalent to using 3000 SGL with percentage uncertainty between 6% to 10%.

For complementary probes SNe Ia and BAO, the simulated next-generation surveys used in this project are Roman and DESI respectively. For SNe Ia, Hounsell et al 2018[7] provided 40 binned simulated z and $\boldsymbol{D}_{\rm stat}$ values and their $\boldsymbol{C}_{\rm sys}$. We generated mock m_B measurements using equation (2) in the standard setting. To account for the variation in the absolute magnitude of each SN Ia event (intrinsic magnitude scattering), for each SN Ia event, we added a small value ϵ randomly drawn from a Gaussian distribution with $\mu = 0$ mag and $\sigma = 0.01$ mag to M_B so that $M_B = -19.2 + \epsilon$ mag. Note that the inclusion of intrinsic magnitude scattering causes a small deviation of the mock universe from the standard setting, and we will discuss this bias and its correction later. For BAO, Font-Ribera et al 2016[8] provided 18 simulated redshifts and σ_{H_z}. We then computed H_z in the standard setting using equation (1).

3.2 LSST single-probe analysis

Before we discuss multiple-probe analysis, it is important to see how a single SGL probe constrain cosmological parameters. We used MCMC sampler in the standard setting on LSST-Like data and fig. 2 shows the constraints we obtained. From the figure, simulated LSST SGL only achieves good constraint on H_0 and partially on w in the neighbourhood of $\Omega_k = 0$. The reason for good constraint on H_0 by SGL is that the combination of angular diameter distances in equation (4) makes $D_{\Delta t}$

approximately inversely proportional to H_0. However, the constraint on Ω_k is not optimistic: $\Omega_k = 0.337^{+0.125}_{-0.317}$. K. C. Wong et al. 2019[1] argued and showed that time-delay distances from SGL are only weakly sensitive to Ω_m and Ω_{de}, and we should expect a similar insensitivity to Ω_k. Therefore, the result that SGL alone imposes weak constraint on Ω_k is not surprising.

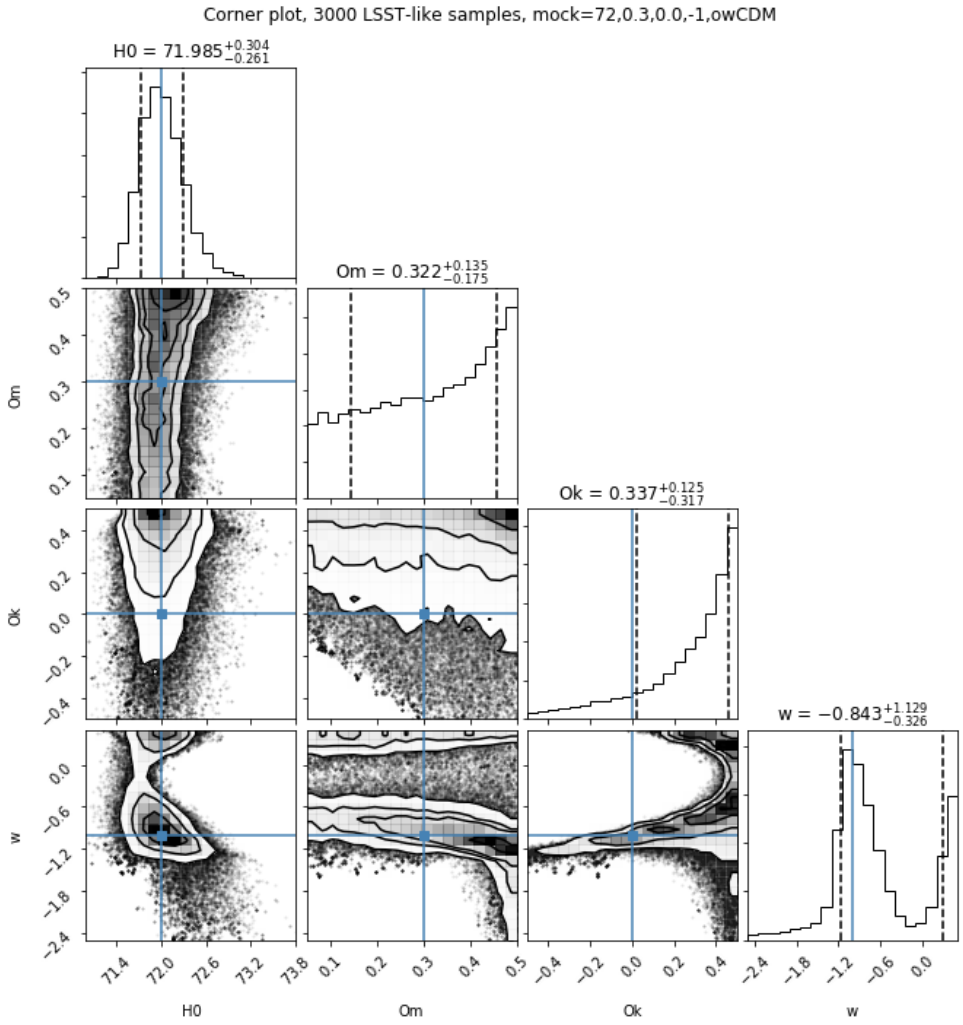

Figure 2: Constraint on parameters by simulated SGL survey LSST

3.3 Bias and correction

While SGL alone is not decent at constraining Ω_k, it is still promising to study how the combined data can complement each other on constraining cosmological parameters. This is especially valuable in view that both SNe Ia and BAO single-probe data failed to impose a strong constraint alone on Ω_k due to w-Ω_k degeneracy. However, in multiple-probe analysis, the inclusion of intrinsic magnitude scattering ϵ in simulated SNe Ia measurements causes a bias on the constraint of cosmological parameters obtained by MCMC sampler in the standard setting. This is because

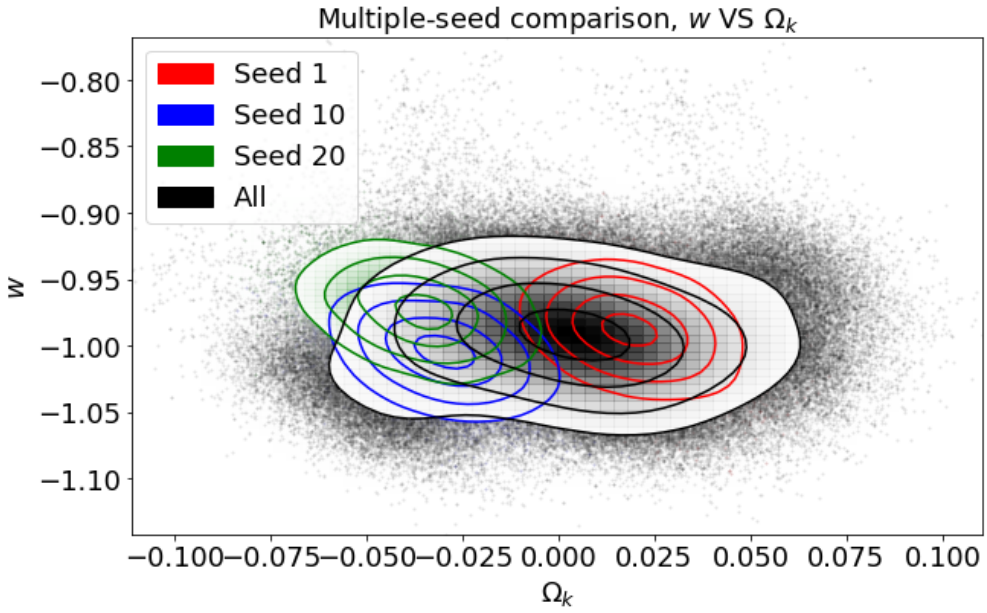

Figure 3: Comparison of w-Ω_k contour with different random seeds

the standard setting has M_B strictly equal to -19.2 mag. However, when we add ϵ drawn from a Gaussian centered at 0 mag, only 40 SNe Ia measurements exist in the binned data source file, and drawing 40 ϵ from the aforementioned Gaussian fall short in creating a fair sample with mean at 0 mag. The magnitude and sign of bias depend on which random seed was used to draw ϵ when applying *numpy.random.seed()* method.

To minimise the bias on the constraint, we used random seeds from integer number 1 to 38 to create 38 samples (no special reasons for 38; 38×40 is a sufficiently large sample size) of SNe Ia measurements, each containing binned data of 40 SNe Ia events. Running MCMC on each SNe Ia sample with the same SGL and BAO measurements and combining all 38 drawn samples of cosmological parameters from MCMC, we could obtain constraints on $H_0, \Omega_m, \Omega_k, w$ and M_B with less or negligible bias. Fig. 3 demonstrates the effect of applying this correction. After obtaining the MCMC samples on cosmological parameters, w VS Ω_k contours for 3 individual seeds (coloured) and all 38 seeds combined (black) are plotted. The center of the black contour has negligible bias from the preset values of $\Omega_k = 0, w = -1$ in the standard setting.

3.4 Multiple-probe analysis

With this bias-correcting step in mind, we used MCMC sampler in the standard setting with intrinsic scattering on each single-probe and multiple-probe next generation data that consist of LSST, Roman and DESI. Then, we plotted a w-Ω_k contour plot for all different combination of probes. Fig. 4. shows the w-Ω_k contour plot we obtained. The wide horizontal span of each single-probe data means that SGL, SNe Ia and BAO all fail to impose strong constraint on Ω_k individually. However, the horizontal-shaped SGL contour (with the implication that SGL constraints w better

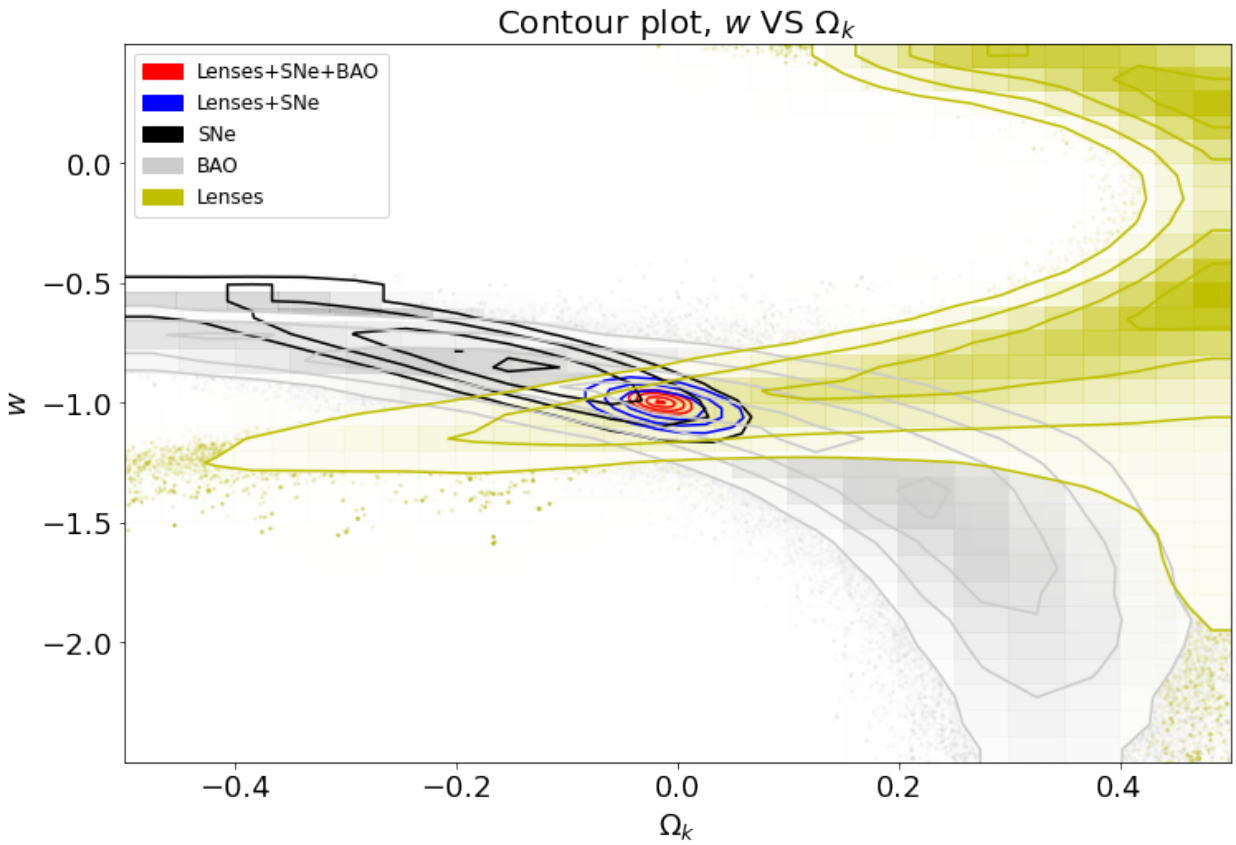

Figure 4: Comparison of w-Ω_k contour for various grouping of probes, with and without SGL

than the other 2 probes in the explored range) 'pierces' into the banana-shaped SNe Ia and BAO contours, creating a small intersection as the region that the final combined constraint locates. We can locate the red contour in fig. 4 and read off the constraint on Ω from a corner plot on the MCMC sample to be: $\Omega_k = -0.003^{+0.014}_{-0.014}$. The inclusion of the horizontal SGL contour helps to break the w-Ω_k degeneracy of SNe Ia and BAO datasets, imposing a strong contraint on Ω_k.

We also used MCMC sampler on LSST+Pantheon data and LSST+Roman+DESI data in non-standard setting. Results of constraints imposed on various parameters in non-standard settings can be found in Appendix A and B.

4 Non-parametric Analysis

4.1 Interpolating Hubble parameter

For non-parametric analysis, we treated the generated $D_{\Delta t}$ and m_B as real simulated measurement data without any assumed model. Specifically, this means that H_z was not given by equation

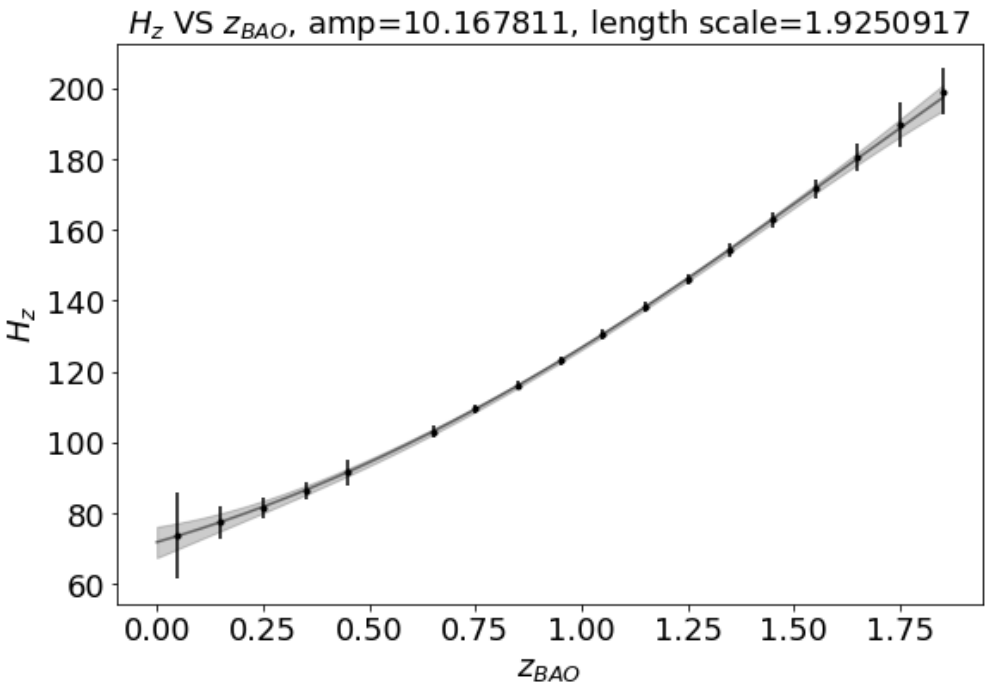

Figure 5: Non-parametric interpolation of H_z with optimal hyper-parameters

(1) but was inferred non-parametrically using BAO data. We used 18 simulated DESI H_z measurement to run GP using python package *george* with squared exponential kernel and optimal hyper-parameters. Using MCMC, we determines the optimal hyper-parameters for this kernel, and they are $a = 10.1678110$ (amplitude) and $l = 1.9250917$ (length-scale) up to 7 s.f.

The outcome of GP is an interpolated curve for H_z between redshift 0 and 1.85 as shown in fig. 5. The solid line is the mean curve of the predictive distribution and the grey zones indicate 1σ standard deviation from the mean curve. This curve of H_z was then used to calculate $E(z)$ which appears in equation (2) & (4) together with the luminosity distance D_L. Take note that $E(z)$ is normalised with respect to $H_0 = 72$ km/s/Mpc, the same as the standard setting in the parametric approach. This enables the previously modelled values in MCMC in equation (4) & (5) to be generated in a non-parametric way in the sense that $E(z)$ is independent of our assumption on dark energy.

4.2 Multiple-probe analysis with GP-fitted Hubble parameter

With our non-parametric inference on $E(z)$, we used MCMC sampler as we did in the parametric approach and obtained the Ω_k-H_0 contour plot shown in fig. 6. The strength and weakness of each probe are most clearly seen in the histograms in fig. 7. We can see that the histograms again corroborates with our previous discussion. SNe Ia has H_0-M_B degeneracy, leading to poor constraints on H_0 and M_B. On the other hand, time-delay distance of SGL give poor constraint on Ω_k, corroborating the result we obtained in the parametric approach. Nevertheless, SGL and

SNe Ia complement each other and the combined data give strong constraints on all 3 parameters H_0, Ω_k and M_B. We state the final result of constraint on curvature by the combined data: $\Omega_k = -0.0004^{+0.0139}_{-0.0142}$. The detailed values of constraints on each parameter with and without SGL in the non-parametric approach can be found in appendix C.

However, adding SGL data in the non-parametric approach gave less significant improvement on constraining Ω_k than that of the parametric approach. This is evident from fig. 7, where the histogram of Ω_k shows similar spread of SGL+SNe curve and SNe curve. This is because in the parametric case, SGL data contribute to the constraint mainly via breaking the w-Ω_k degeneracy, while in the non-parametric case there is no such degeneracy to break. Instead, SGL data break the H_0-M_B degeneracy in SNe Ia data and indirectly contribute to constraining Ω_k.

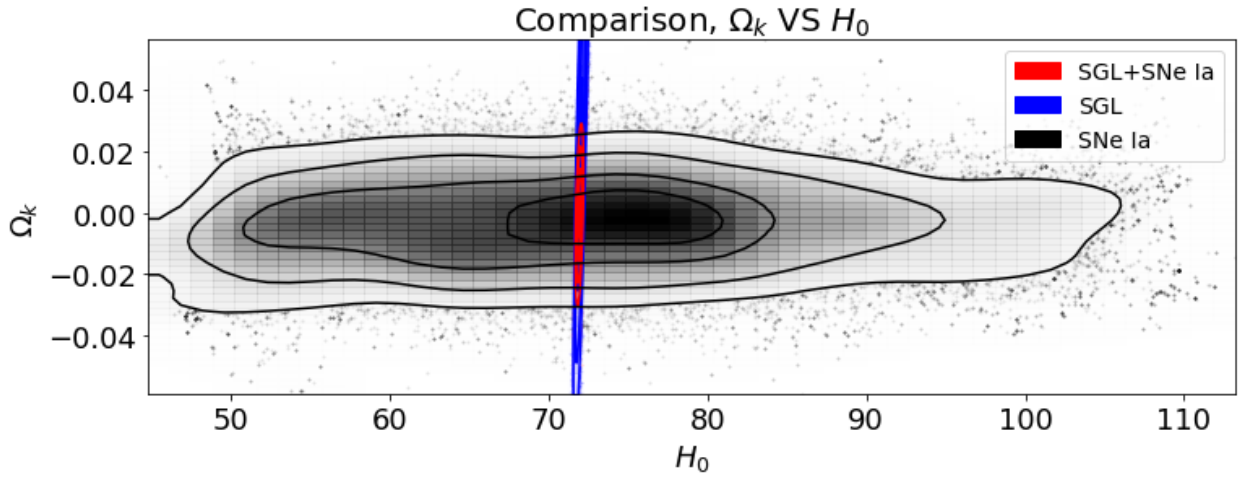

Figure 6: Comparison of Ω_k-H_0 contour in non-parametric analysis, with and without SGL

5 Conclusion

In this project, we explored the ability of SGL to complement SNe Ia and BAO on constraining Ω_k via both parametric and non-parametric approaches. Result shows optimistic forecast on adding SGL into analysis to get stronger constraint on Ω_k. In the parametric approach with an assumed owCDM model of the universe, when combining SGL with simulated next-generation SNe and BAO surveys, the constraint obtained is: $\Omega_k = -0.003^{+0.014}_{-0.014}$. This is a significant stronger constraint as compared to the constraints imposed by single-probe data. In the non-parametric approach, the constraint achieved is: $\Omega_k = -0.0004^{+0.0139}_{-0.0142}$.

Although SGL failed to impose a strong constraint on Ω_k alone, when we combined SGL with other probes explored in this project, we all obtained stronger constraints on Ω_k. This is because SGL data complement the weakly constrained parameters of other probes, hence improving the constraint achieved on all parameters overall. It will be promising to study what constraint on Ω_k can be achieved when combining SGL with other consistent and complementary probes, as well

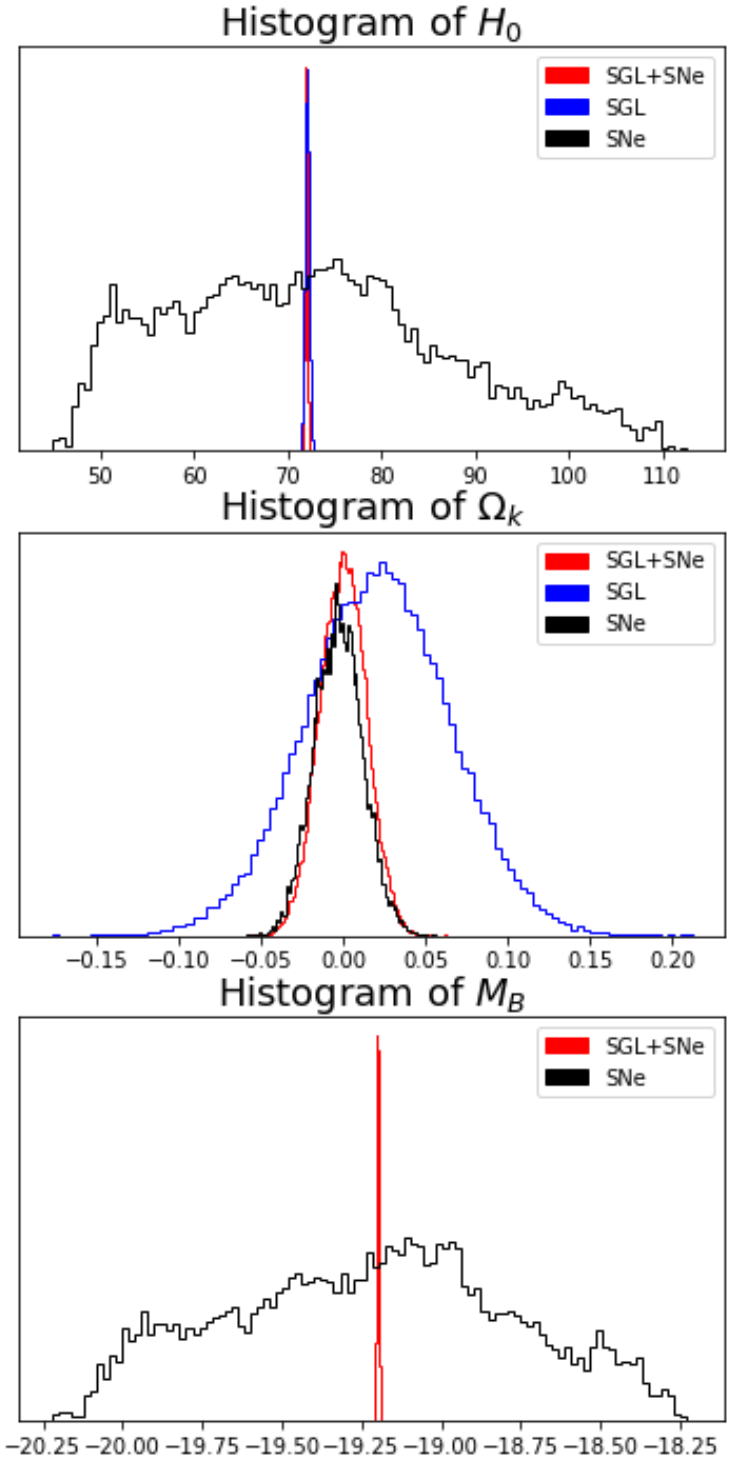

Figure 7: Histograms of parameters by MCMC with and without SGL

as analysis with more complicated model of the universe such as ow_0w_aCDM and slow-roll model. Hopefully, this project can serve as an elementary but instructive forecast on using next-generation surveys to constrain Ω_k.

References

[1] Kenneth C. Wong et al. "H0LiCOW – XIII. A 2.4 per cent measurement of H0 from lensed quasars: 5.3σ tension between early- and late-Universe probes". In: *Monthly Notices of the Royal Astronomical Society* 498.1 (Sept. 2019), pp. 1420–1439. DOI: 10.1093/mnras/stz3094. URL: https://doi.org/10.1093/mnras/stz3094.

[2] Huber, S. et al. "Strongly lensed SNe Ia in the era of LSST: observing cadence for lens discoveries and time-delay measurements". In: *A&A* 631 (2019), A161. DOI: 10.1051/0004-6361/201935370. URL: https://doi.org/10.1051/0004-6361/201935370.

[3] D. M. Scolnic et al. "The Complete Light-curve Sample of Spectroscopically Confirmed SNe Ia from Pan-STARRS1 and Cosmological Constraints from the Combined Pantheon Sample". In: *The Astrophysical Journal* 859.2 (May 2018), p. 101. DOI: 10.3847/1538-4357/aab9bb. URL: https://dx.doi.org/10.3847/1538-4357/aab9bb.

[4] C. E. Rasmussen & C. K. I Williams. *Gaussian processes for machine learning*. MIT Press, 2005.

[5] Suhail Dhawan, Justin Alsing, and Sunny Vagnozzi. "Non-parametric spatial curvature inference using late-Universe cosmological probes". In: *Monthly Notices of the Royal Astronomical Society: Letters* 506.1 (June 2021), pp. L1–L5. DOI: 10.1093/mnrasl/slab058. URL: https://doi.org/10.1093/mnrasl/slab058.

[6] LSST Dark Energy Science Collaboration (LSST DESC) et al. "The LSST DESC DC2 Simulated Sky Survey". In: ApJS 253.1, 31 (Mar. 2021), p. 31. DOI: 10.3847/1538-4365/abd62c. arXiv: 2010.05926 [astro-ph.IM].

[7] R Hounsell et al. "Simulations of the WFIRST supernova survey and forecasts of cosmological constraints". In: *The Astrophysical Journal* 867.1 (2018), p. 23.

[8] Kyle S Dawson et al. "The SDSS-IV extended Baryon Oscillation Spectroscopic Survey: overview and early data". In: *The Astronomical Journal* 151.2 (2016), p. 44.

Appendix A

Constraints on parameters with simulated LSST and Pantheon

Cosmological model		H_0	Ω_m	Ω_k	w	M_B
1000 *SGL + SNe Ia*						
$o\Lambda$CDM	Mock	72	0.3	0.00	-1	-19.2
	MCMC	$71.906^{+0.324}_{-0.327}$	$0.312^{+0.047}_{-0.048}$	$-0.039^{+0.118}_{-0.110}$	$\equiv -1$	$-19.207^{+0.018}_{-0.018}$
2000 *SGL + SNe Ia*						
$o\Lambda$CDM	Mock	72	0.3	0.00	-1	-19.2
	MCMC	$71.939^{+0.254}_{-0.255}$	$0.307^{+0.039}_{-0.040}$	$-0.024^{+0.093}_{-0.090}$	$\equiv -1$	$-19.205^{+0.016}_{-0.016}$
3000 *SGL + SNe Ia*						
$o\Lambda$CDM	Mock	72	0.3	0.00	-1	-19.2
	MCMC	$71.959^{+0.212}_{-0.215}$	$0.304^{+0.035}_{-0.035}$	$-0.017^{+0.080}_{-0.076}$	$\equiv -1$	$-19.205^{+0.015}_{-0.015}$
$o\Lambda$CDM	Mock	72	0.3	0.03	-1	-19.2
	MCMC	$71.952^{+0.210}_{-0.211}$	$0.304^{+0.035}_{-0.035}$	$0.010^{+0.081}_{-0.078}$	$\equiv -1$	$-19.205^{+0.015}_{-0.015}$
$o\Lambda$CDM	Mock	72	0.3	0.05	-1	-19.2
	MCMC	$71.953^{+0.211}_{-0.211}$	$0.304^{+0.035}_{-0.036}$	$0.030^{+0.084}_{-0.080}$	$\equiv -1$	$-19.205^{+0.015}_{-0.015}$
$o\Lambda$CDM	Mock	72	0.3	-0.03	-1	-19.2
	MCMC	$71.954^{+0.212}_{-0.214}$	$0.304^{+0.034}_{-0.035}$	$-0.048^{+0.078}_{-0.075}$	$\equiv -1$	$-19.205^{+0.015}_{-0.015}$
$o\Lambda$CDM	Mock	72	0.3	-0.05	-1	-19.2
	MCMC	$71.954^{+0.213}_{-0.213}$	$0.304^{+0.034}_{-0.034}$	$-0.066^{+0.076}_{-0.072}$	$\equiv -1$	$-19.205^{+0.015}_{-0.015}$
owCDM	Mock	72	0.3	0	-1	-19.2
	MCMC	$72.059^{+0.285}_{-0.275}$	$0.337^{+0.071}_{-0.076}$	$-0.058^{+0.122}_{-0.113}$	$-1.043^{+0.087}_{-0.078}$	$-19.205^{+0.015}_{-0.015}$
3000 *SGL*						
FwCDM	Mock	72	0.3	0	-1	-
	MCMC	$71.997^{+0.319}_{-0.287}$	$0.313^{+0.131}_{-0.162}$	$\equiv 0$	$-1.029^{+0.063}_{-0.081}$	-

No. of binned SNe Ia events = 40

No. of walkers in MCMC = 32

No. of samples in MCMC = 20000

numpy.random.seed() used in random processes without bias-correcting step: 20

Appendix B

Constraints on parameters with simulated LSST, Roman and DESI

Cosmological model		H_0	Ω_m	Ω_k	w	M_B
SGL						
owCDM	Mock	72	0.3	0	-1	-
	MCMC*	$71.985^{+0.304}_{-0.261}$	$0.322^{+0.135}_{-0.175}$	$0.337^{+0.125}_{-0.317}$	$-0.843^{+1.129}_{-0.326}$	-
SNe Ia						
owCDM	Mock	72	0.3	0	-1	-19.2
	MCMC	$74.121^{+28.898}_{-20.841}$	$0.302^{+0.033}_{-0.074}$	$-0.156^{+0.121}_{-0.150}$	$-0.829^{+0.155}_{-0.167}$	$-19.111^{+0.713}_{-0.718}$
BAO						
owCDM	Mock	72	0.3	0	-1	-
	MCMC	$72.738^{+5.279}_{-3.941}$	$0.246^{+0.096}_{-0.078}$	$0.180^{+0.166}_{-0.351}$	$-1.215^{+0.382}_{-0.658}$	-
SGL + SNe Ia						
$o\Lambda$CDM	Mock	72	0.3	0	-1	-19.2
	MCMC	$71.957^{+0.112}_{-0.112}$	$0.317^{+0.005}_{-0.005}$	$-0.017^{+0.018}_{-0.017}$	$\equiv -1$	$-19.192^{+0.007}_{-0.007}$
owCDM	Mock	72	0.3	0	-1	-19.2
	MCMC	$72.004^{+0.259}_{-0.261}$	$0.318^{+0.007}_{-0.008}$	$-0.012^{+0.028}_{-0.028}$	$-1.008^{+0.042}_{-0.044}$	$-19.191^{+0.009}_{-0.009}$
SGL + SNe Ia + BAO						
$o\Lambda$CDM	Mock	72	0.3	0	-1	-19.2
	MCMC	$71.905^{+0.100}_{-0.101}$	$0.315^{+0.005}_{-0.005}$	$-0.031^{+0.013}_{-0.013}$	$\equiv -1$	$-19.201^{+0.004}_{-0.004}$
owCDM	Mock	72	0.3	0	-1	-19.2
	MCMC1*	$71.787^{+0.148}_{-0.148}$	$0.313^{+0.006}_{-0.006}$	$-0.036^{+0.014}_{-0.014}$	$-0.974^{+0.024}_{-0.024}$	$-19.199^{+0.004}_{-0.004}$
owCDM	Mock	72	0.3	0	-1	-19.2
	MCMC2*	$72.170^{+0.155}_{-0.164}$	$0.296^{+0.006}_{-0.006}$	$0.014^{+0.014}_{-0.015}$	$-1.028^{+0.027}_{-0.026}$	$-19.201^{+0.004}_{-0.004}$
owCDM	Mock	72	0.3	0	-1	-19.2
	MCMC3*	$71.954^{+0.145}_{-0.150}$	$0.306^{+0.006}_{-0.006}$	$-0.015^{+0.014}_{-0.014}$	$-0.997^{+0.024}_{-0.024}$	$-19.202^{+0.004}_{-0.004}$

No. of (equivalent) SGL events = 3000

No. of binned SNe Ia events = 40

No. of BAO measurements = 18

No. of walkers in MCMC = 32

No. of samples in MCMC = 20000

* MCMC & MCMC1 indicate seed=20, MCMC2 indicates seed=21, MCMC3 indicates seed=22

Appendix C

Constraint on parameters in non-parametric analysis

Probe		H_0	Ω_k	M_B
SNe Ia	Mock	72	0	-19.2
	MCMC	$71.692^{+16.381}_{-15.366}$	$-0.003^{+0.015}_{-0.015}$	$-19.208^{+0.447}_{-0.522}$
SGL	Mock	72	0	-
	MCMC	$72.055^{+0.221}_{-0.223}$	$0.021^{+0.043}_{-0.043}$	-
SGL+SNe Ia	Mock	72	0	-19.2
	MCMC	$71.954^{+0.124}_{-0.124}$	$-0.0004^{+0.0139}_{-0.0142}$	$-19.200^{+0.003}_{-0.003}$

No. of (equivalent) SGL events = 3000

No. of binned SNe Ia events = 40

No. of walkers in MCMC = 32

No. of samples in MCMC = 8000